



HAL
open science

Development of polymer films and biological matrices standards for selenium, mercury and endogenous elements quantitative LA-ICP MS imaging in entire rainbow trout fry

Laurie Labeyrie, Germain Vallverdu, Dominique Michau, Stéphanie Fontagné-Dicharry, Sandra Mounicou

► To cite this version:

Laurie Labeyrie, Germain Vallverdu, Dominique Michau, Stéphanie Fontagné-Dicharry, Sandra Mounicou. Development of polymer films and biological matrices standards for selenium, mercury and endogenous elements quantitative LA-ICP MS imaging in entire rainbow trout fry. *Microchemical Journal*, 2023, 194, pp.109204. 10.1016/j.microc.2023.109204 . hal-04197105

HAL Id: hal-04197105

<https://hal.science/hal-04197105>

Submitted on 14 Sep 2023

HAL is a multi-disciplinary open access archive for the deposit and dissemination of scientific research documents, whether they are published or not. The documents may come from teaching and research institutions in France or abroad, or from public or private research centers.

L'archive ouverte pluridisciplinaire **HAL**, est destinée au dépôt et à la diffusion de documents scientifiques de niveau recherche, publiés ou non, émanant des établissements d'enseignement et de recherche français ou étrangers, des laboratoires publics ou privés.

Development of polymer films and biological matrices standards for selenium, mercury and endogenous elements quantitative LA-ICP MS imaging in entire rainbow trout fry

Laurie Labeyrie¹, Germain Salvato Vallverdu¹, Dominique Michau², Stéphanie Fontagné-Dicharry³, Sandra Mounicou¹

¹Université de Pau et des Pays de l'Adour, E2S UPPA, CNRS, IPREM, Pau, France

²CNRS, Université Bordeaux, ICMCB, UMR 5026, 87 avenue du Dr A. Schweitzer, 33608, Pessac, France

³INRAE, Université de Pau et des Pays de l'Adour, E2S UPPA, NUMEA, 64310 Saint-Pée-sur-Nivelle, France

* Author to whom correspondence should be addressed: sandra.mounicou@univ-pau.fr, IPREM UMR 5254, Technopôle HélioParc, 2 avenue du Président Angot, 64053 Pau cedex 09, phone: ++33 5 59 40 77 64

Abstract

The quantitative imaging of trace elements in biological samples can bring information on their assimilation pathways and help understanding their toxicity or essentiality. This study presents the development of two quantitative LA-ICP MS methodologies and their comparison for Se, Hg, Cu, Zn and Mo imaging in rainbow trout. The first method is based on spiked polymer films (dextran) allowing internal standardization with Ge and Te. The second method relies on the matrix-matched standards (MMS) methodology, with homogenized and spiked trout muscle and calf liver. For Se, Cu, Zn and Mo, linear regressions with correlation coefficient above 0.994 were obtained by LA-ICP MS analysis for both methods. For Hg, only MMS calibration provided linear regression as polymer films exhibited Hg unstable signals during LA-ICP MS analysis. Element concentrations spiked in muscle and liver MMS were also confirmed by ICP MS and used to validate the polymer films method as values obtained for Se, Hg, Mo and Cu were in good agreement. While LODs of polymer film method were in the range of 0.06-0.6 $\mu\text{g}\cdot\text{g}^{-1}$ for Cu, Se, Mo, and 5 $\mu\text{g}\cdot\text{g}^{-1}$ for Zn, values were higher for MMS method (from 0.06 (Mo) to 2.2 (Cu) $\mu\text{g}\cdot\text{g}^{-1}$, and 30 of $\mu\text{g}\cdot\text{g}^{-1}$ for Zn). Particular attention has been paid to sample embedding and water was found to minimize internal standard response bias. Both methods were then applied to the quantitative mapping of these five elements in rainbow trout fry supplemented or not with organic forms of Se and Hg through parental and direct feeding. Calibrations were analysed before and after sample imaging evidencing a lower bias between the two quantifications with polymer films calibration than with MMS calibration. For the first time, elements concentrations were determined at 60 x 60 μm spatial resolution in specific tissues or organs of entire fry. Depending on the element, polymer films quantification was in agreement with trout muscle (Cu, Se) or with calf liver MMS quantification (Zn).

Keywords

LA-ICP MS, bioimaging, selenium, mercury, quantification, trout fry

1 Introduction

Selenium (Se) is an essential oligo-element known for its antioxidant properties as it is included in selenoproteins such as glutathione peroxidases (GPX) [1]. It is used as a supplement in aquaculture feeds to promote fish growth performance and welfare. However, Se metabolism is not fully understood and vary depending on its bioavailability (i.e. chemical form). A number of studies have been carried over rainbow trout (*Oncorhynchus mykiss*) to determine the impact of Se level and forms used on trout Se assimilation (ICP MS analysis of whole-body fry) and antioxidative status (enzyme expression) [2,3]. Furthermore, mercury (Hg) is of concern as it can be contained into fishmeal and ingredients of alternative diets under development. Knowing its antagonistic character toward Se, Hg might modify Se bioavailability and thus decrease Se benefit for fish health [4]. To go further, the determination of the localisation of Se and Hg in the different organs and tissues would bring information into mechanisms of assimilation of Se and potential interactions with Hg.

Laser-Ablation Inductively Coupled Plasma Mass Spectrometry (LA-ICP MS), with its spatial resolution (μm) and high sensitivity ($\mu\text{g}\cdot\text{g}^{-1}$ and below) is a suitable technique to study element distribution in biological samples. Wischhusen *et al.* studied the localisation of Se in rainbow trout fry thin sections by LA-ICP MS after parental and direct supplementation with sodium selenite or hydroxy-selenomethionine [3]. Preferential bioaccumulation of Se in specific organs or tissues according to the Se form could be evidenced, and quantitative imaging data would have been a great added value for the accurate comparison between the different diets conditions.

Trace elements quantification in biological samples by LA-ICP MS is complex as already discussed in the literature[5]. Indeed, elemental fractionation and matrix effects are often observed and have to be compensated by an adequate calibration. Although more and more methods are being developed, they must be adapted to the sample problematics. The use of CRMs would be ideal, but they are not available for all kind of fresh biological samples and all chemical elements. Nevertheless, in case of dry sample analysis, CRMs can be modified to match the elements concentration range of the sample of interest if the matrix is suitable [6]. Matrix-matched standards (MMS) can also be fully prepared in laboratory by using the same matrix as the sample, or at least a similar one [7,8]. The main drawback of this methodology is the time-consuming standard preparation protocols for tissue and spiking homogenisation. So, non-MMS have been developed such as spiked gelatin [9] and agarose gel [10], or standard elements introduced into a polymer films like polymethylmethacrylate (PMMA) [11] and dextran films [12], and also into spiked inks for patterns printing [13].

In addition to external calibration, the use of an internal standard appears to be necessary as signal drifts caused by a sensibility loss, ablation and transport variations can happen during long imaging sessions. Some studies have used an homogeneously and endogenous element but this situation is rather scarce. Also ^{13}C which was used several times [14,15], has a higher first ionization potential than most of the elements studied and appears to be released in the gas form, whereas metallic elements are in the particulate form [16]. In other studies, internal standard was added via solution nebulization [17] or directly below or onto the sample section to allow for ablation process variation correction. For example, gold has been sputtered at the surface of the sample [18]. Furthermore, as for external calibration, spiked ink can be printed onto the section [19], or samples can be deposited onto gelatin gel spiked with internal standards [20]. Similarly, the section can be placed above polymer films prepared by spin-coating. Austin *et al.* used PMMA spiked with organic copper (Cu) and zinc (Zn) [11] and Arnaudguilhem *et al.* used dextran spiked with a wide range of elements [12].

Very recently, for Hg and Se quantitative LA-ICP MS imaging in mushrooms, Braeuer *et al.* used standards made of gelatin and L-cysteine deposited as droplets onto glass slides [21]. To assess the validity of the calibration, they prepared a reference material with homogenized mushroom. Ogra *et*

al. carried out Hg quantitative imaging in rat kidney and liver by means of a home-made Hg-spiked rat liver calibration standards [22].

The aim of this study was to quantitatively map Se and Hg as well as other endogenous elements such as Cu, Zn and molybdenum (Mo) in fish fry thin sections of ca 3 cm long by using internal standardization and external calibration. For that purpose, a first method was developed and based on the one of Arnaudguilhem *et al.*, which allow the use of internal standardization and external calibration with dextran films [12]. The method was adapted and optimized for larger glass slides (4 cm x 4 cm) to enable deposit of entire fish sections. This implied the full characterization of the films (element concentration, thickness, mass). This method was compared to a developed MMS methodology using spiked and homogenized trout muscle and calf liver for external calibration. Thin sections of MMS were deposited onto polymer films allowing internal standardization. Metals concentrations in produced MMS were determined by ICP MS and by LA-ICP MS using the polymer films calibrations enabling methodologies comparison and accuracy verification. For the first time, calibrations obtained by both methods were applied for the quantitative imaging of Se, Hg and three endogenous elements (Cu, Zn and Mo) in aquaculture rainbow trout fed with different meals, supplemented or not with organic Se and Hg forms.

2 Materials and methods

2.1 Reagents

Dextran polymer (Mw of ca. 500 000 g.mol⁻¹) was purchased from VWR (Fontenay-sous-Bois, France). Elemental solutions at 50 000 mg.L⁻¹ (Cu and Zn), 10 000 mg.L⁻¹ (Se, Mo and Hg) and 1 000 mg.L⁻¹ (Ge and Te, used as internal standards) were purchased from SCP Science (PlasmaCAL, Courtaboeuf, France). Intermediate solutions were prepared in 2% ultrapure HNO₃ (69-70% ULTRATRACE PPB GRADE, Scharlau, Atlantic Labo, Bruges, Belgium). All solutions and experiments were prepared with Milli-Q water (resistivity ≥ 18.2 Ω cm) obtained from a Milli-Q Elix water purification system (Millipore, Molsheim, France).

2.2 Instrumentation

An Agilent 7700x model (Agilent Technologies, Tokyo, Japan) mounted with Ni cones and Micromist nebulizer (for liquid samples analysis) was used. The detection parameters were optimized and mass calibration checked using a solution of 1 µg.L⁻¹ of Li, Y, Ba, Tl and Ce in 2% HNO₃. For laser ablation analysis, the detector was then coupled to a laser ablation system (NWR 213, ESI, Fremont, CA, USA). Helium was used at 800 mL.min⁻¹ to transport the ablated material through a TV2 ablation cell and mixed with argon before introduction to the ICP dry plasma. The detection parameters (torch position, lenses) were then adjusted with a NIST 612 glass standard (NIST, Washington, USA). Additional information are given in table S1.

2.3 Preparation of polymer thin film standards

As for the original method [12], solution of dextran was prepared in water at 60 mg.mL⁻¹. It was then spiked with different concentrations of metallic solutions to produce calibration standards: from 0 to 60 µg.g⁻¹ for Se, Mo and Hg, and from 0 to 300 µg.g⁻¹ for Cu and Zn. Internal standards (Ge and Te) were added in each solution at 10 µg.g⁻¹ for signal normalization. A solution containing only internal standards was also prepared to be used as substrate for samples and matrix-matched standards deposit after spin-coating. The proportion of dextran was the same for every calibrant and sample substrate and the final volume was adjusted with water.

As films support, 4 x 4 cm glass slides were custom-made (Verre Vagner, Toulouse, France) with soda-lime glass. Before their use, they were soaked in a 2% HNO₃ bath, rinsed with water, cleaned with

ethanol and Kimtech paper, and particles were removed by pressurized air. Then, approximately 2 mL of each solution were filtered through 0.45 μm cellulose filter (VWR, Fontenay-sous-Bois, France) and deposited onto the glass slides. Spin-coating (Polos SPIN150i spin-coater model, SPS, Vourles, France) parameters were optimized to produce homogeneous films on larger slides than the previous method [12] and were set as followed: 4500 rpm for 60s with a vacuum pressure of 46 kPa.

Each glass slide was weighed with ultrahigh precision balance (Automated-S microbalance XP6, Mettler Toledo, Viroflay, France) before and after the spin-coating step to determine the mass of each film. Their thickness was determined by profilometry using a WYKO NT1100 Optical profiling System (Veeco, Dourdan, France) after scratching the film to the glass with a scalpel. One film per concentration was used and the mean value was calculated.

2.4 Preparation of matrix-matched tissue standards

Each standard was spiked with 120 μL of metallic solutions to produce four levels of theoretical final concentrations and including two ranges, i.e. 0, 12.5, 50, 200 $\mu\text{g}\cdot\text{g}^{-1}$ for Cu and Zn, and 0, 2.5, 10, 40 $\mu\text{g}\cdot\text{g}^{-1}$ for Se, Mo, Hg.

Trout muscle was bought from a supermarket and cut into pieces. A large quantity was pre-ground with an Ultra-Turrax (IKA T10 basic, Imlab, Lille, France) in a 50 mL tube. Some was crushed for 40 min at 20 Hz with a ball mill (MM 200, Retsch, Haan, Germany). Then, 5 g of finely ground muscle was transferred to a 10 mL tube, spiked with 120 μL of metallic solution and homogenized with the Ultra-Turrax. Two tubes were prepared and then gathered and homogenized. The spiked matrix was finally compacted in two 2 mL Eppendorf tubes and placed at $-80\text{ }^{\circ}\text{C}$.

Calf liver was bought from a supermarket. First, it was pre-ground with a kitchen blender. Then 2 x 5 g were spiked with 120 μL of metallic solutions and homogenized in 10 mL tubes with an Ultra-Turrax. Both tubes were then gathered and homogenized again. Spiked liver was finally compacted in two 2 mL Eppendorf tubes and placed at $-80\text{ }^{\circ}\text{C}$.

Of the 2 Eppendorf tubes prepared for each matrix, one was reserved for cryomicrotomy before LA-ICP MS analysis and the other one for total metal analysis by ICP MS.

2.5 Standards and samples cutting by cryomicrotomy

2.5.1 Matrix-matched standards

Trout muscle and calf liver standards were taken out of Eppendorf tubes in the cryomicrotome chamber (CM 1950 model, Leica, France). The blocks were fixed on the specimen disc of the cryomicrotome and embedded directly onto it with water. Chamber/sample holder temperatures were set to $-15\text{ }^{\circ}\text{C}/-18\text{ }^{\circ}\text{C}$ for trout muscle standards and to $-20\text{ }^{\circ}\text{C}/-20\text{ }^{\circ}\text{C}$ for calf liver. Thin sections of 8 μm were produced and deposited on glass slides covered with polymer films containing internal standards for signal normalization.

2.5.2 Trout samples

All procedures to obtain trout samples were performed in compliance with the European Directive 2010/63/EU for the protection of animals used for scientific purposes and the French Decree no. 2013-118 for animal experimentation. The feeding trial for broodstock and fry stages was approved by the Ethical Committee C2EA-73 and the French Ministry of Higher Education and Research (reference number APAFIS #32548-2021072309475577 v5) and performed in the INRAE experimental facilities of Lées-Athas and Donzacq (France, <https://doi.org/10.15454/GPYD-AM38>). The rainbow trout broodstock were fed one of six experimental diets designed to differ in Se form and content and Hg

level. The diets were given for 6 months prior to spawning. At spawning, oocytes from each spawning female were collected through stripping, pooled, and fertilized with a pool of sperm retrieved from males of the same dietary treatment collected on the same day. The eggs were cultivated until swim-up fry stage. At swim-up fry stage, the pooled progeny of each parental treatment was subdivided into different fry feeding groups and given one of four fry plant-based diets designed at similar Se and Hg levels compared with the broodstock diets for 3 weeks.

The quantitative imaging was applied to two trout fry raised with different conditions of feeding. The broodstock of the first fry was fed with a control plant-based diet and the fry received a plant diet supplemented with Hg and Se. The broodstock of the second fry was fed with a plant diet supplemented with Hg and Se and the fry was fed with the control plant-based. The control plant-based diets was not supplemented with Se and Hg, having a basal Se level of $0.2 \mu\text{g}\cdot\text{g}^{-1}$ diet. For the supplemented plant diets, Se was given as L-selenomethionine (Excellent Selenium 4000, Orffa, Breda, Netherlands) at $4 \mu\text{g Se}\cdot\text{g}^{-1}$ diet and Hg was given as methylmercury(II) chloride (Sigma-Aldrich, Saint-Quentin-Fallavier, France) at $2 \mu\text{g Hg}\cdot\text{g}^{-1}$ diet. After 3 weeks of feeding with fry diets, fry were euthanized with an overdose of benzocaine, frozen in liquid nitrogen and stored at -80°C .

Before being fixed to the specimen disc, fishtail of fry were cut to fit the disc (uninteresting part of the fish). Cryomicrotome chamber/sample holder temperatures were set to $-15^\circ\text{C}/-18^\circ\text{C}$. Fry were embedded in water, cut into $8 \mu\text{m}$ sections and deposited on polymer films containing the internal standards. Fish central part was chosen, where we could see all organs. The sections were stored in boxes and analysed a maximum of 3 days after their cutting.

2.6 Standards' metal concentration determination by ICP MS

2.6.1 Polymer films

Glass slides were weighed before and after the spin-coating step. 5 films per concentration were placed in plastic boxes, previously washed 3 times with 2% HNO_3 and rinsed with H_2O . 7 mL of 2% HNO_3 were added to cover each glass slide and boxes were placed onto a stirring plate overnight for film solubilization. Glass slides were rinsed twice with 2% HNO_3 and analysed by LA-ICP MS to be sure of the complete release of metals in solutions. All the solutions (solubilization and rinses) were analysed by ICP MS and concentrations were calculated by considering the mass of each film.

2.6.2 Matrix-matched standards (MMS)

For each standard of both matrices, 3 portions of approximately 150 mg (exact mass weighed) and 2 mm thickness were recovered from one Eppendorf tube: one at each extremity and one at the centre of the block. They were digested in 400 μL of 69% HNO_3 during 280 min at 80°C into a heating block (Digiprep, SCP Sciences). Acid content was then reduced to 2% with water.

2.6.3 ICP MS analysis of liquid samples

For ICP MS analysis, H_2 was used (between 3.8 and 4 $\text{mL}\cdot\text{min}^{-1}$) as collision gas to lower interferences on ^{63}Cu , ^{65}Cu , ^{64}Zn , ^{66}Zn , ^{78}Se and ^{80}Se . External calibration ($0\text{-}20 \mu\text{g}\cdot\text{L}^{-1}$) and standard addition were used in addition to internal normalization (with ^{209}Bi) for element quantification. Integration time for each isotope were 90 ms.

2.6.4 LA-ICP MS analysis and calibration

The same analytical conditions were used for both standards and samples. A square laser spot of $60 \times 60 \mu\text{m}$ was used for standards and fish samples, lines were scanned with a speed of $90 \mu\text{m}\cdot\text{s}^{-1}$ and a laser shot repetition rate of 20 Hz. The distance between ablated lines of fish sample (size of ca 3×1

cm) was 60 μm . The power of the laser was adjusted to have an energy between 3.5 and 6.5 $\text{J}\cdot\text{cm}^{-2}$ to ablate the entire thickness of tissue and film while minimizing the ablation of the surface glass slide. ^{63}Cu , ^{64}Zn and ^{202}Hg were monitored with an integration time of 0.08 s, 0.1 s for ^{78}Se , ^{80}Se and ^{98}Mo , and 0.05 s for ^{125}Te and ^{72}Ge , leading to a total sampling time of 0.658 s.

For calibration using polymer thin film, between 2 and 3 lines of approximately 2.5 cm long were scanned. For the calibration using MMS, between 2 and 4 lines were scanned across the entire width of the sections. For both calibration method, the intensities of each ion were normalized to the internal standards signals and the average was calculated. A calibration curve could be produced for each element in which the normalized intensities are given as a function of the concentrations determined by ICP MS.

An ICP MS acquisition file (csv format) was obtained for each scanned line. For imaging experiment, a Python homemade program was used to produce an image representing elements concentrations per pixel with a colour code after blank subtraction and calibration.

3 Results and discussion

1. 1. Polymer thin films

3.1.1 Characterization

Films were produced on glass slides of 4 x 4 cm to be able to deposit samples between 2 and 3.5 cm long. For spin-coating, 2 types of glass were tested: borosilicate and soda-lime in the desired custom-made dimension. Borosilicate slides needed to be pyrolyzed and well cleaned in nitric acid before being able to produce films on their surface. Even with this glass preparation, films were not always homogeneous and 62% of the produced film substrates were discarded. However, with soda-lime glass, a better film homogeneity could be obtained and the preparation was repeatable. Then, soda-lime glass was chosen. The production of the glass, which is poured on a tin bath, results in a difference in surface composition depending on the side of the slide. Both sides were analysed by LA-ICP MS to determine potential contamination of the surfaces and the bare side was slightly contaminated with Ge. Then, films were created on the tin coated side of the glass. Mass, thickness of each film and metal concentrations are presented in the supplementary information (**Table S2**).

Masses of the films were determined by the weight of 8 glass slides before and after the spin-coating step (**Table S1**). The values obtained here are in accordance with our previous study [12] in which 2.3 times smaller glass slides were used which lead to masses proportionally lighter. Also, higher masses were obtained for the most concentrated standard and the lowest for the blank. It could be explained by a slight difference in the nitric acid content of the solutions. The 300 / 60 $\mu\text{g}\cdot\text{g}^{-1}$ film standard contained the highest volume of spiking solution, which lead to more nitric acid in the final solution (0.4%), and the blank contained only the internal standard solution, which lead to less nitric acid (0.1%). As expected from the masses, thicknesses similar to Arnaudguilhem *et al.* were obtained with a mean value of 60 ± 10 nm (excluding the thickness of the 50 / 10 $\mu\text{g}\cdot\text{g}^{-1}$ film standard which appears as an unexplained outlier).

The comparison of these concentrations with the theoretical ones, allowed us to determine preconcentration factors between 17 and 36 (average of ca 20), preconcentration occurring during spin-coating process due to solvent evaporation as already reported [12] [11]. In our previous work, we determined a factor between 12 and 18 for Cu, Zn, Se and Mo [12], while Austin *et al.* [11] obtained a factor around 10 for Cu and Zn under different polymer containing solutions. Here, the factors were slightly higher, especially for Cu and Zn but still in the same order of magnitude. The difference may be due to a different pressure applied during spin-coating to maintain the larger glass slide than in our

previous conditions. This emphasizes the need to properly characterise the chemical composition of the films as a slight variation of an experimental parameter impacts the film characteristics.

Contrary to our previous work [12] where Hg was lost during spin-coating process, we were able to determine a preconcentration factor for Hg. This may be explained by a difference in the content of the polymer solutions which is less complex than in the previous study, which seems to help in the stabilization of Hg during the spin-coating solution. However, the Hg concentration in the films was not repeatable, leading to high standard deviation values compared to the other elements. The exact elements concentration of each film determined by ICP MS are used to plot calibration curves.

3.1.2 LA-ICP MS calibration curves

The choice of internal standards was made by considering their mass and/or their ionization potential, which should be closed to those of the elements of interest, and their absence from the biological samples investigated. This led us to consider germanium (Ge) and tellurium (Te) as potential internal standards. Indeed, Ge (M=72.63 u) has a mass close to the one of Cu (M=63.55 u), Zn (M=65.38 u), Se (M=78.97 u) and Mo (M=95.95 u), and a first ionization potential (FIP=7.90 eV) close to the one of Cu (FIP=7.73 eV) and Mo (FIP=7.09 eV). Te has a first ionization potential (FIP=9.01 eV) close to the one of Zn (FIP=9.39 eV), Se (FIP=9.75 eV) and to a less extent to Hg (FIP=10.31eV).

The homogeneity of the film could be verified by calculating the relative standard deviation (RSD) of the signals of three spaced scans of ca 2.5 cm long on one blank standard. Values of 11% for Ge and 15% for Te were obtained. The RSD between two films was 10% and 8% for Ge and Te, respectively. In our previous study, when scanning a large surface on 2.6 x 2.6 cm slides, RSD of internal standards was around 9% for two films analysed, and the RSD between the two films was in the range 10-14% [12]. Here, the same calibration was analysed 10 times (10 different days) and the RSDs of the signals of the internal standards for each film (n=2-3 scans) was calculated: average values of 13% for Ge and 16% for Te were obtained. The homogeneity of the Ge and Te was similar for all film standards and the increase of the concentration of the other elements had no impact.

For the elements of interest (Cu, Zn, Se, Mo and Hg), RSDs of the signals on one film (n=2-3 scans, 10 calibration analysis considered for average values) were increasing when their concentration was decreasing, except for Zn for which it was around 9% for all standards. They were varying from 11% for the most concentrated standard to 35% for the 2.5 / 0.5 $\mu\text{g}\cdot\text{g}^{-1}$ standard for Cu, from 13% to 40% for Se and from 11% to 21% for Mo. When applying internal standardization, RSDs were very slightly higher for all standards elements. After normalization to Ge signals, RSDs were of 14% for the most concentrated standard to 39% for the least concentrated one for Cu, from 15% to 42% for Se, from 14% to 25% for Mo, and around 13% for Zn. Signals normalization to Te continued to slightly increase RSDs: 18% for the most concentrated standard to 39% for the least concentrated standard for Cu, from 19% to 44% for Se, from 17% to 26% for Mo, and around 17% for Zn.

Austin et al. [11] obtained RSDs of Cu and Zn signals below 10% after normalization to Y and Ru with PMMA spin-coated films and organic solutions. However, smaller surfaces were analysed (25 x 25mm quartz slides), and an organic soluble polymer spiked with only 4 elements was used, which differs from our solutions.

Homogeneous films could be produced on larger glass slides (4 x 4 cm) than in the previous method [12] which allows to depose and analyse samples of several cm long without cutting them, and to obtain linear calibration curves. Calibration with good correlation coefficients (0.996 to 1, 0.999 average) could be produced for Cu, Zn, Se and Mo regardless of normalization. Calibration curves obtained for one day of analysis are presented in **Fig. 1S** of the supplementary information (for Hg,

data are shown later in **Fig. 1**). For all elements, greater slopes were obtained under Te normalization than with Ge normalization due to lower Te intensity compare to Ge.

For a long period of analysis (i.e 10 days) on the same films, RSDs of the calibration slopes were calculated and values of 10%, 4%, 3% and 6% were respectively obtained for Cu, Zn, Se and Mo after signal normalization with Ge, and 13%, 6%, 4% and 9% after normalization with Te. Without normalization, RSDs were 27%, 21%, 22% and 21%, showing that these elements are suitable as internal standards. Normalization with Ge signals reduces slightly RSDs but not significantly. The stability of the films could be assessed by analysing the same calibration six months after its preparation. The slopes difference was lower than 5.2% for Cu, Zn, Se and Mo after normalization to both internal standards (**Fig. 2S**, supplementary information). The repeatability of the film preparation could be assessed by preparing and analysing two different set of calibrations standards at 6 months apart. Each set was analysed 9 times. RSDs of the slopes of the 18 calibration curves of 9% were obtained for Cu and Mo, and 13% for Zn, after normalization to Ge (against 28% and 29% for Cu and Mo, and 17% for Zn after Te normalization). A RSD of 8% was obtained for Se (78 and 80) after normalization to Te (against 24% after Ge normalization). These low RSDs show that this method is repeatable and that Ge internal standard is more suited for Cu and Mo while Te plays a better role for Se normalization. This is likely to be explained by the closed FIP and mass between Cu, Mo and Ge. FIP is readily the dominant factor to compensate for Se sensitivity drift. Not as Se, Zn tends to be affected similarly regardless of Ge or Te normalization, most likely reflecting an intermediate situation, i.e medium mass and high FIP, but both lower than the Se ones.

The calibration curves for Hg were not reproducible. The RSDs of the calibration slopes obtained during 10 different days of analysis were above 70%. The correlation coefficients were not as good as for the other elements and were between 0.642 and 0.981 (0.897 in average). Moreover, the signals were instable (as wave pattern over the line scan) during LA-ICP MS film analysis. Hg stabilisation tests in solution and during spin-coating were done by adding ligands such as cysteine, β -mercaptoethanol or gold to the polymer solution, but no improvement was noticed in terms of signal stability (wave pattern still observed).

3.2 Matrix-matched tissue standards

3.2.1 Characterization

Different animal tissues were bought from a supermarket and investigated as potential standards: monkfish liver, chicken liver, calf liver and trout muscle. Chicken liver was too liquid to be cut by cryomicrotomy. The inter individual variability of the texture of monkfish liver (too liquid or too fatty) prevented us from cryo-sectioning it after different methods of freezing. Calf liver and trout muscle were suitable for standard preparation as proper tissue homogenisation could be performed. Basal metal concentrations and after spiking at 3 levels in each trout muscle and calf liver standard were determined by ICP MS (**Table 1**).

Table 1. Elements concentrations in trout muscle and calf liver standards determined by ICP MS. Theoretical values are given for Cu and Zn (0 to 200 $\mu\text{g.g}^{-1}$) and for Se, Mo and Hg (0 to 40 $\mu\text{g.g}^{-1}$). Ge and Te are internal standards.

Theoretical concentration	Standard matrix	Experimental concentration ($\mu\text{g.g}^{-1}$)
---------------------------	-----------------	---

Cu, Zn / Se, Mo, Hg ($\mu\text{g}\cdot\text{g}^{-1}$)		Cu	Zn	Se	Mo	Hg
0 ($\mu\text{g}\cdot\text{g}^{-1}$)	Trout muscle	0.4 ± 0.1	3 ± 1	0.12 ± 0.01	0.0046 ± 0.0004	0.022 ± 0.003
	Calf liver	233 ± 14	41 ± 2	0.49 ± 0.01	0.71 ± 0.01	0.0072 ± 0.0003
12.5 / 2.5 ($\mu\text{g}\cdot\text{g}^{-1}$)	Trout muscle	14 ± 1	18 ± 2	2.7 ± 0.2	2.6 ± 0.1	2.3 ± 0.5
	Calf liver	270 ± 28	59 ± 8	2.9 ± 0.1	3.3 ± 0.2	2.7 ± 0.5
50 / 10 ($\mu\text{g}\cdot\text{g}^{-1}$)	Trout muscle	51 ± 2	60 ± 2	10 ± 1	9.9 ± 0.2	9 ± 1
	Calf liver	286 ± 23	82 ± 2	9.9 ± 0.5	10.7 ± 0.5	8.6 ± 0.3
200 / 40 ($\mu\text{g}\cdot\text{g}^{-1}$)	Trout muscle	215 ± 15	217 ± 29	42 ± 4	41 ± 4	28 ± 5
	Calf liver	676 ± 174	266 ± 45	41 ± 3	43 ± 2	47 ± 9

In raw tissues, Te was below the LOD ($0.0003 \mu\text{g}\cdot\text{g}^{-1}$) and Ge was present at very low concentration in calf liver that is not detectable by LA-ICP MS ($0.0011 \pm 0.0002 \mu\text{g}\cdot\text{g}^{-1}$). Concentrations determined by ICP MS analysis were close to the theoretical values and proportionality between each standard was found for Se and Mo for both matrices, for Cu and Zn for trout muscle and for Hg for calf liver. However, basal Cu concentration is naturally high [23], and too high to consider calf liver for Cu LA-ICP MS MMS. This matrix also naturally contains Zn, ($41 \mu\text{g}\cdot\text{g}^{-1}$ in the control) but concentrations between standards are quite proportional. Moreover, as not expected, Hg concentration in the $40 \mu\text{g}\cdot\text{g}^{-1}$ trout muscle standard is a 1.4 fold lower than the theoretical value. A loss during the sample preparation could have happened. In general, these data show that the sample preparation (homogenization and spiking) is appropriate and allows to obtain homogeneous standards (RSDs of concentrations between 2 and 21%).

3.2.2 LA-ICP MS calibration curves

Linear calibration curves ($0.9917 < R^2 < 0.9999$ for the examples shown in **Fig. 3S** in SI) could be obtained for all elements from thin section MMS of both matrices, except for Cu as it could be expected from the total concentrations determined by ICP MS. Considering LA-ICP MS analysis over a 6-month period, average R^2 were between 0.994 and 0.997 for Se, Hg, Cu and Mo. The lowest linearity was for Zn with an average R^2 between 0.980 and 0.990. The LA-ICP MS data show the greatest sensitivity when normalizing all elements intensity with Te as for polymer film internal standards calibration.

The stability of the methodology was assessed by calculating RSDs of the slopes of calibration curves obtained during 9 different days of analysis. For trout muscle, RSDs were in the range of 10% (Zn), 16%

(Se, Mo) and 32% (Hg) regardless of the internal standard used while stability of Cu slope was of 12% after Ge normalisation (against 17% with Te). Using calf liver MMS, a significant decrease in terms of stability could be noticed, as RSDs increased up to ca 40% (Zn), 23% (Se), 33% (Mo), 40% (Hg) and with very similar behaviour for the two internal standards. As the analysis of these two matrix standards were done at the same time, the stability results indicate that the standard matrix plays a role in the stabilization of the spiked elements in the homogenized tissues. This statement was confirmed by considering the mean slope of 11 calibration curves for both matrices, where Zn showed the highest difference between the two mean slope (31%) compared to Hg (2%), Se (15%) and Mo (17%). The data underline as well the greatest vulnerability of Hg in terms of stability over time in the standard.

As for polymer films, an analysis session was done under high laboratory temperature (i.e. > 25°C) and it showed a reduction of the variation of the slopes when Cu and Mo signals are normalized with Ge for both matrices and when Se (78 and 80) signals are normalized to Te signals. For Zn, the slope difference was lower with normalization to Ge for both matrices, while Te normalization minimized variation of Zn slope obtained from polymer film. For Hg, the difference between slopes was similar with both normalizations for trout muscle and was lower with Ge normalization for calf liver. In case of atypical atmospheric conditions of analysis, Ge should be chosen as internal standard.

Contrary to the polymer films, linear calibration curves could be obtained (**Fig. 1**) for Hg with MMS ($0.994 < \text{average } R^2 < 0.996$).

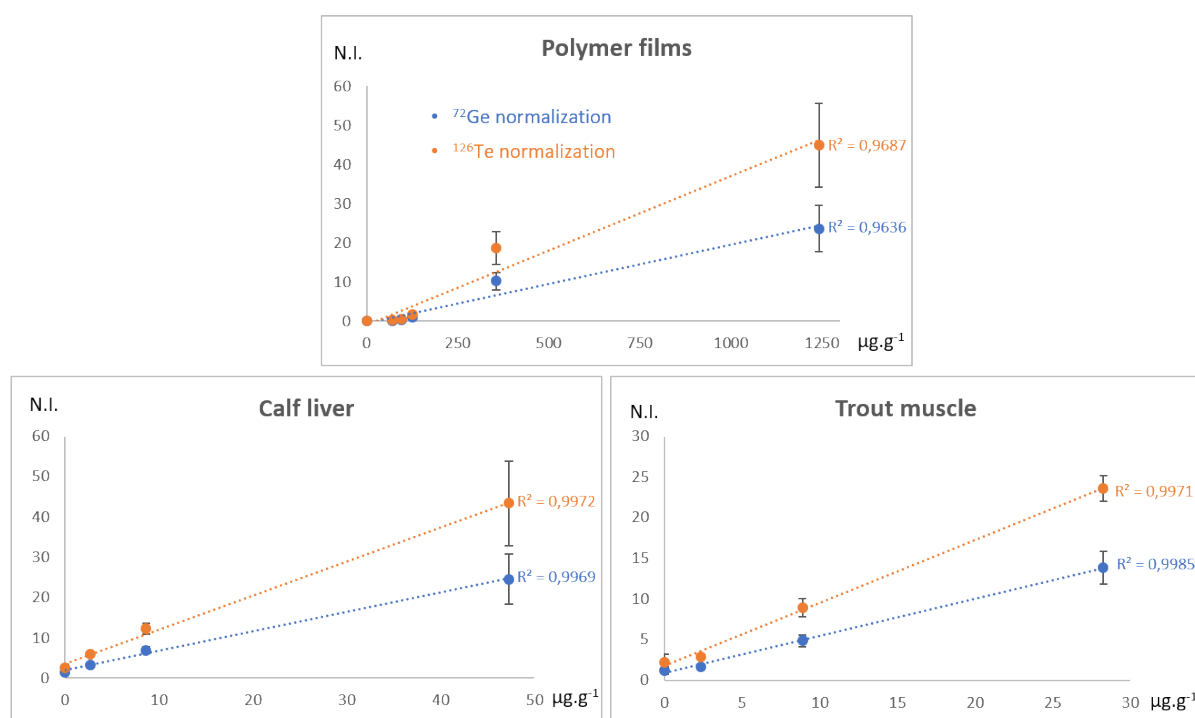


Fig. 1. Examples of Hg calibration curves obtained by the LA-ICP MS analysis of polymer films, of trout muscle and of calf liver standards. Intensities are normalized by ^{72}Ge or by ^{126}Te , and are plotted as a function of the experimental concentrations.

Even if we paid particular attention for homogenized tissue compression, the fresh MMS sections still contain cracks, also due to the high water content (like in real samples). This causes an important variability of the signals of the elements of interest, leading to RSDs on one scan of several tens of

percent (only intensities above the background signal were integrated). Homogeneity problems and cracked standards sections have already been reported [20] [22]. RSDs of ^{72}Ge and ^{126}Te signals on one scan were around 30% on average for both matrices ($n = 132$ scans).

The potential difference in LA-ICP MS response between a fresh section and a dried section (analysed several days after its cutting) was assessed. Calibrations obtained with freshly cut standards were compared to calibrations obtained with 5-day-old sections and no significant difference was observed. It may be due to the high He flow crossing the ablation cell that causes the drying of the fresh section rapidly.

3.3 Impact of embedding media

To be analysed by LA-ICP MS, MMS and samples had to be embedded in a media to maintain their integrity during sectioning. Three embedding media were experimented, i.e. carboxymethylcellulose (CMC), the regular OCT and water. The different images of ^{72}Ge and ^{126}Te during the analysis of trout fry embedded with the different media are presented in **Fig. 2** and facing the images of ^{78}Se . Initially and in view of setting up a correlative imaging experiment 5% CMC used for Matrix-Assisted Laser Desorption/Ionization coupled to Mass Spectrometry (MALDI-MS) imaging [24] was tested but important matrix effects were noticed. Indeed, internal standards signal considerably dropped when laser was scanning the resin and we could observe that the polymer film was less ablated compared to zones without resin. On **Fig. 2 A** and **B**, film disturbance can be observed around the fish section due to the presence of resin. So, our efforts were focused on the choice of the embedding media leading to less matrix effects. An attempt consisted in decreasing the CMC content to 2%, but the same phenomenon was still observed. Even so the regular OCT (QPath, VWR) minimized this effect, it was still present. No matrix effects were observed during LA-ICP MS analysis when water was used as embedding media, and the quality of the cutting was similar than with the other resins. No degradation of the tissue's morphology could be observed after sectioning. The MMS and samples were therefore embedded with water for further experiments.

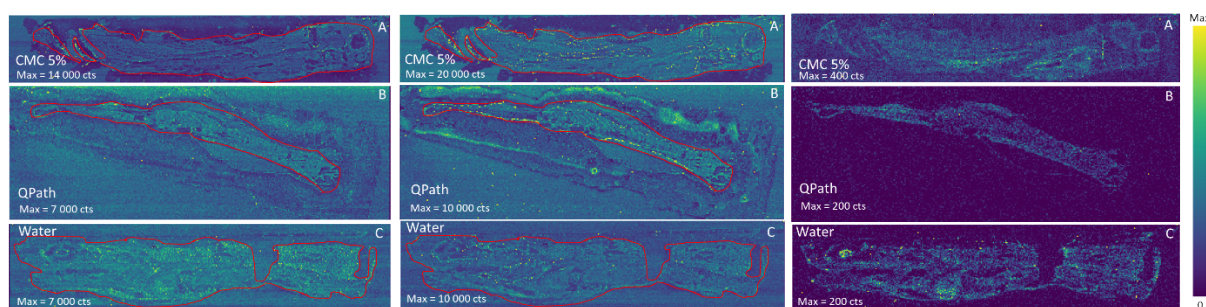


Fig. 2. ^{126}Te (left), ^{72}Ge (centre) and ^{78}Se (right) imaging when analysing trout fry (whole body for A and C, or just a part for B) of the same feeding condition embedded with CMC 5% (A), with QPath (B) and with water (C) – A was analysed during a different session from B and C explaining the different signal intensities (highest for A sample). The red lines surround the fishes. Film retractation is observed (through internal standard signal) around the fishes for CMC and QPath embedding.

3.4 Polymer film method verification and methods comparison

For the polymer film methodology, limits of detection (LOD) were determined with the linear regression, by considering 3 times the standard deviation of the blanks ($\text{LOD} = 3\text{SD}/\text{slope}$) and by considering the density of the polymer film (2.9271), the thickness of the film (60 nm) and the thickness of the tissue section (8 μm). For the MMS methodology, LOD were calculated with the linear regressions obtained for trout muscle and calf liver and with the respective blanks. LODs obtained with the polymer films method and the MMS are presented in **Fig. 3**.

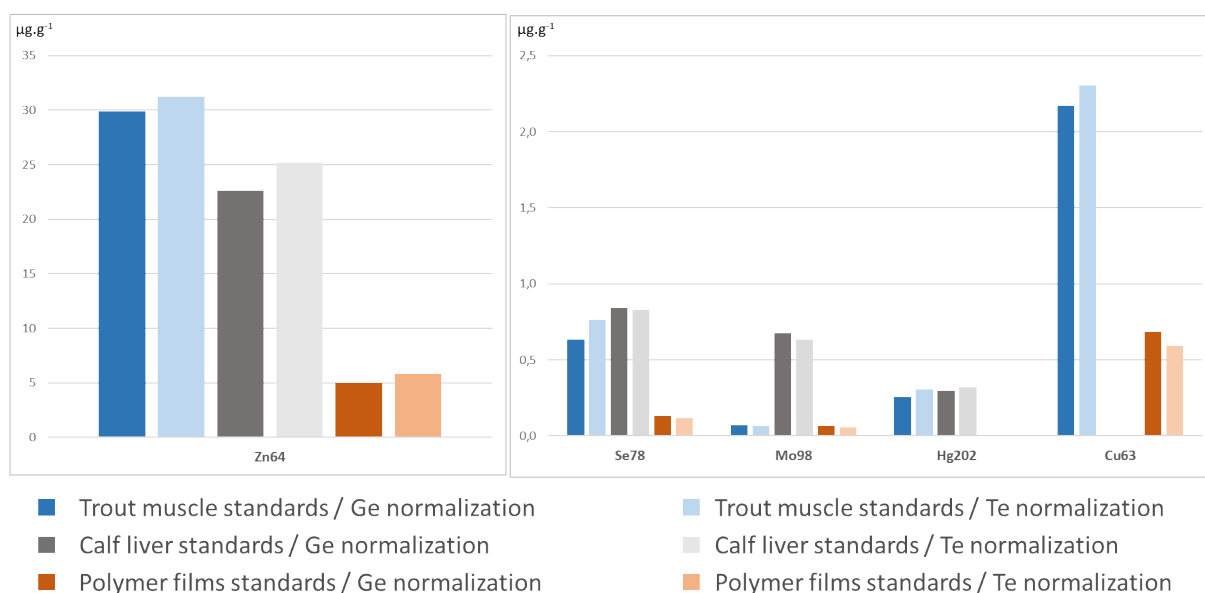


Fig. 3. Limits of detection ($\mu\text{g}\cdot\text{g}^{-1}$) obtained with the polymer films standards (orange), with trout muscle standards (blue) and with calf liver standards (grey), and after Ge normalization (darkest colour) and Te normalization (lightest colour).

LODs were lower with the polymer films than with the MMS. It is explained by the better homogeneity of the films compared to the MMS and led to lower SDs. Moreover, LODs were higher for calf liver (except for Hg) as it naturally contained Zn, Se and Mo [25]. For Cu, LOD of $0.7/0.6 \mu\text{g}\cdot\text{g}^{-1}$ (Ge normalization/Te normalization) could be obtained with polymer films, and was almost 4 times higher with trout muscle standards. LOD of $1.8 \mu\text{g}\cdot\text{g}^{-1}$ was attained by Bishop *et al.* with sheep brains analysed by LA-ICP-QQQ-MS and H_2 as collision gas [26] and we reached $0.3 \mu\text{g}\cdot\text{g}^{-1}$ under He reaction gas during our former study [12]. For Zn, LOD around $5 \mu\text{g}\cdot\text{g}^{-1}$ was obtained with polymer films although it is about 5 times higher than in our former work using He as reaction gas [12]. This value was high but expected as the presence of Zn was detected in glass slide. With MMS, the LODs were around $30 \mu\text{g}\cdot\text{g}^{-1}$. This high value was expected for calf liver as $41 \mu\text{g}\cdot\text{g}^{-1}$ of Zn were quantified by ICP MS in the control standard. However, for trout muscle, it was supposed to be lower as only $3 \mu\text{g}\cdot\text{g}^{-1}$ were found in the control. This high LOD is explained by matrix effects, which causes drops in the signals and then high SDs. Regarding the literature, LOD of $3.6 \mu\text{g}\cdot\text{g}^{-1}$ was attained by Bishop *et al.* when using sheep brains, which differs in Zn natural content (analysed by LA-ICP-QQQ-MS + H_2) [26]. For Mo, LOD was $0.07/0.06 \mu\text{g}\cdot\text{g}^{-1}$ (Ge normalization/Te normalization) with polymer films and with trout muscle matrices. However, it was 10 times higher with calf liver. The value obtained with polymer films was close to the one of our previous study; no other LODs were reported for this element. For ^{78}Se , LOD of $0.1 \mu\text{g}\cdot\text{g}^{-1}$ could be obtained with the polymer films with both normalization, which is slightly better than the one reported by Brauer *et al.* with gelatin-cysteine microdroplets standards ($0.3 \mu\text{g}\cdot\text{g}^{-1}$) [21]. Additionally, this value is 10 times lower than the one we obtained in our previous study ($1 \mu\text{g}\cdot\text{g}^{-1}$) with He as collision gas [12]. This shows again the greatest benefit of H_2 for Se analysis compared to He. Bishop *et al.* already showed that adding H_2 as reaction gas allowed to improve the LOD of ^{78}Se , from $0.93 \mu\text{g}\cdot\text{g}^{-1}$ without gas to $0.31 \mu\text{g}\cdot\text{g}^{-1}$ (with sheep brain standards and ICP-QQQ-MS) [26]. Here, with MMS, higher LODs ($0.6\text{--}0.8 \mu\text{g}\cdot\text{g}^{-1}$ with both normalization) were obtained compared to the polymer films method but it is still much better than the one found ($15.3 \mu\text{g}\cdot\text{g}^{-1}$) with spiked-brain standards [27]. However, much lower values ($0.03 \mu\text{g}\cdot\text{g}^{-1}$) could be reached with brain standards and an ICP-QQQ-MS [28]. For Hg, LODs were around $0.3 \mu\text{g}\cdot\text{g}^{-1}$ with MMS, which is much lower than what Debeljak *et al.* obtained with Hg-spiked embedding medium standards ($4.9 \mu\text{g}\cdot\text{g}^{-1}$) [29] and what Pozebon *et al.* obtained ($2.2 \mu\text{g}\cdot\text{g}^{-1}$) [27]. However, low values of $0.04 \mu\text{g}\cdot\text{g}^{-1}$ and even $0.006 \mu\text{g}\cdot\text{g}^{-1}$ could be obtained with liver and gelatin-cysteine standards analysed by ICP MS/MS [22] [21]. To sum up, LODs for all elements were lower

using the polymer film standards compared to MMS. This shows the inconvenience of using biological matrices as standards as they can naturally contain elements under study. On the other side, MMS allowed Hg calibration, which was impossible with polymer films standards.

The variation of the methodology sensitivity (RSD calibration slopes) was more important using MMS (up to 41%) than polymer film standards (up to 13%) during 10 days of analysis. Similarly, Ge and Te signals vary more for MMS (30% RSD, $n = 132$ scans) than polymer films (15% RSD, $n = 198$ scans). This is explained by a better homogeneity of the films compared to the muscle and liver sections that are cracked and/or to a higher inertia of polymer films that are already dried once they are produced contrary to the fresh MMS. Moreover, better linearity was obtained with the polymeric films, which is likely due to the easier sample preparation and spiking of polymer solutions than homogenisation and spiking of fresh tissue.

Trout muscle and calf liver standards were quantified by means of the polymer films calibration curves. Data normalized by either Ge or Te were similar, so only one normalization (Ge) is presented in **Fig. 4**.

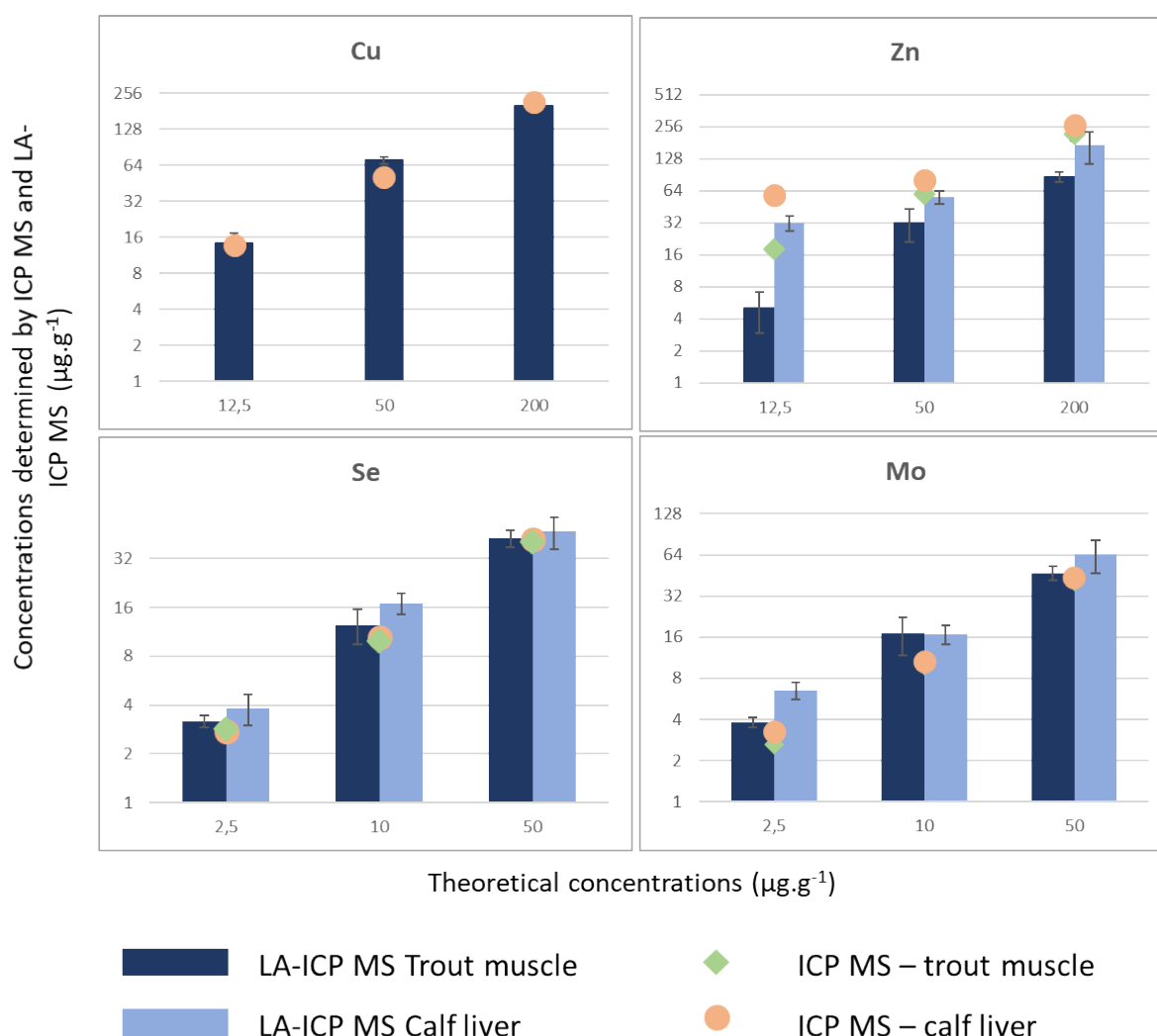


Figure 4. Metal concentrations determined by LA-ICP MS with the polymer films method (histogram) and by ICP MS (dots) in trout muscle (LA-ICP MS: dark blue; ICP MS: green) and calf liver (LA-ICP MS: light blue; ICP MS: orange) standards (log scale), $n = 11$ analysis.

Concentrations determined by LA-ICP MS with polymer films are slightly higher than the ones obtained by ICP MS for Se and Mo for both matrices, and for Cu with trout muscle. This can be explained by the drying of the sections caused by the He flow going through the ablation cell and thus concentrating the chemical elements in the section. However, concentrations determined for Zn for both matrices and for each standard are between 1.5 to 3.6 times lower than the ICP MS value which may be explained by high Zn level in LA-ICP MS blanks and matrix effect in trout muscle. For Cu in trout muscle, the bias between the LA-ICP MS concentration and the ICP MS value is of only 4% for the 12.5 $\mu\text{g}\cdot\text{g}^{-1}$ standard and of 6% for the 200 $\mu\text{g}\cdot\text{g}^{-1}$, but is higher for the 50 $\mu\text{g}\cdot\text{g}^{-1}$ standard (37%). For Se in trout muscle, LA-ICP MS and ICP MS values are really close with differences of 16%, 20% and 1% for 2.5, 10 and 40 $\mu\text{g}\cdot\text{g}^{-1}$ standards respectively. For calf liver, the LA-ICP MS concentrations are within 2 standard deviations. For Mo, LA-ICP MS and ICP MS concentrations are within 1 to 1.3 standard deviations for the 10 and 50 $\mu\text{g}\cdot\text{g}^{-1}$ trout muscle standard. For the three others standards, values are within 2.1 to 3.5 standard deviations. For all elements, the concentrations of the control standards determined by LA-ICP MS differs more from the ICP MS value as they are closed to the LODs.

All these results show that the use of polymer films as calibrants allows to reach really good performances, with low LODs (except for Zn) and linear calibration curves (except for Hg) on large glass slides of 4 x 4 cm and allow quantification in muscle and liver standards with good accordance with ICP MS values. Also, their main advantage is their easiest and quicker preparation compared to trout muscle and calf liver standards, which have to be really well homogenized and are more prone to contaminations. However, Hg quantification by polymer film was not possible. Moreover, trout muscle and calf liver standards allowed to produce linear calibrations curves for all elements including Hg. For both method, internal standardization allowed to correct for slopes differences between different days of analysis.

3.5 *Application to trout fry from aquaculture*

Both quantification methods were applied to the quantitative imaging of Se, Hg, Cu, Zn and Mo in two trout fry with different feeding conditions. Fry 1 was fed a diet supplemented with MeHg and SeMet but not its broodstock. The broodstock of the fry 2 was supplemented with MeHg and SeMet and fry 2 was fed a diet without any Hg or Se supplementation. Quantitative images are presented in the **Fig. 5**. To minimize bias for quantification, calibration was done just before and after sample imaging. Concentrations shown were obtained with the MMS method for Hg and with polymer films for the other elements.

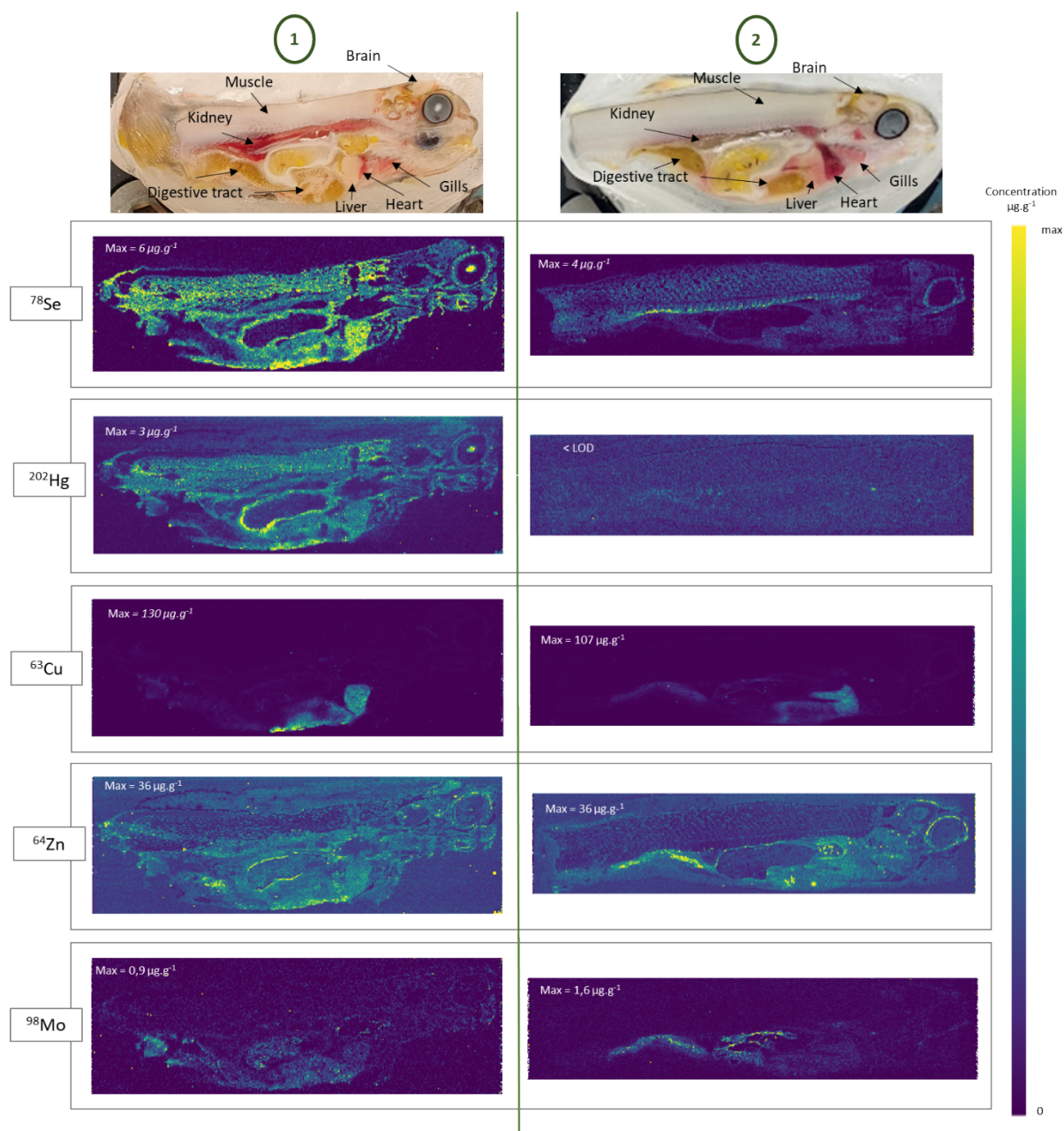


Figure 5. Quantitative images of ^{78}Se , ^{202}Hg , ^{63}Cu , ^{64}Zn and ^{98}Mo in $8\ \mu\text{m}$ section of 2 rainbow trout fry fed with different aquafeeds. Fry 1 (left): dietary Se and Hg supplementation directly to the fry. Fry 2 (right): parental Se and Hg supplementation through broodstock feeding. All images are normalized to ^{72}Ge signals. Top: photographs of specimens before sectioning.

Direct dietary Se supplementation to the fry leads to a concentration up to $6\ \mu\text{g.g}^{-1}$ in the muscle, the liver, and some parts of the intestines. When the supplementation is only parental, $4\ \mu\text{g.g}^{-1}$ can be reached in the muscle and the kidney, but the concentration is lower in the intestines and in the liver, between 1 and $2\ \mu\text{g.g}^{-1}$. For both fry, Se is also found in the eye periphery and in the brain, at a higher concentration in fry 1 compared to fry 2. Direct Hg supplementation clearly leads to a higher concentration in the fry compared to parental supplementation. Hg is found around $2\ \mu\text{g.g}^{-1}$ in the muscle, the kidney, the liver and intestines, and at $1\ \mu\text{g.g}^{-1}$ in the brain. However, no Hg was found when the supplementation was only parental (confirmed by two other replicates). This might let us hypothesize that Hg is not transferred from the broodstock to the progeny with such dietary ranges ($2\ \mu\text{g.g}^{-1}$). Hg was found to co-localize with Se in all the body of fry 1. To note as well, the signal tailing of Hg as already reported by Debeljak *et al.* and associated to the formation of vapour causing the

deposition of Hg in the ablation cell and tubing, and its slow desorption [29]. The washout time can also be improved by optimizing the instrumental device [30], which can be part of a future amelioration. For both fry, Cu was mainly found in the digestive tract and the liver. More than 100 $\mu\text{g}\cdot\text{g}^{-1}$ was determined in the intestines and was twice lower in the liver. Zn had a similar localisation and concentration for both fry, between 20 to 40 $\mu\text{g}\cdot\text{g}^{-1}$ in the intestines and the liver. However, this value must be higher given that the concentrations determined in muscle and liver standards were underestimated. Zinc was also found in the periphery of the eyes. Molybdenum was localized in intestines and the liver of both fry, up to 1 $\mu\text{g}\cdot\text{g}^{-1}$ in the first fry, and slightly higher (up to 1.6 $\mu\text{g}\cdot\text{g}^{-1}$) in the second fry.

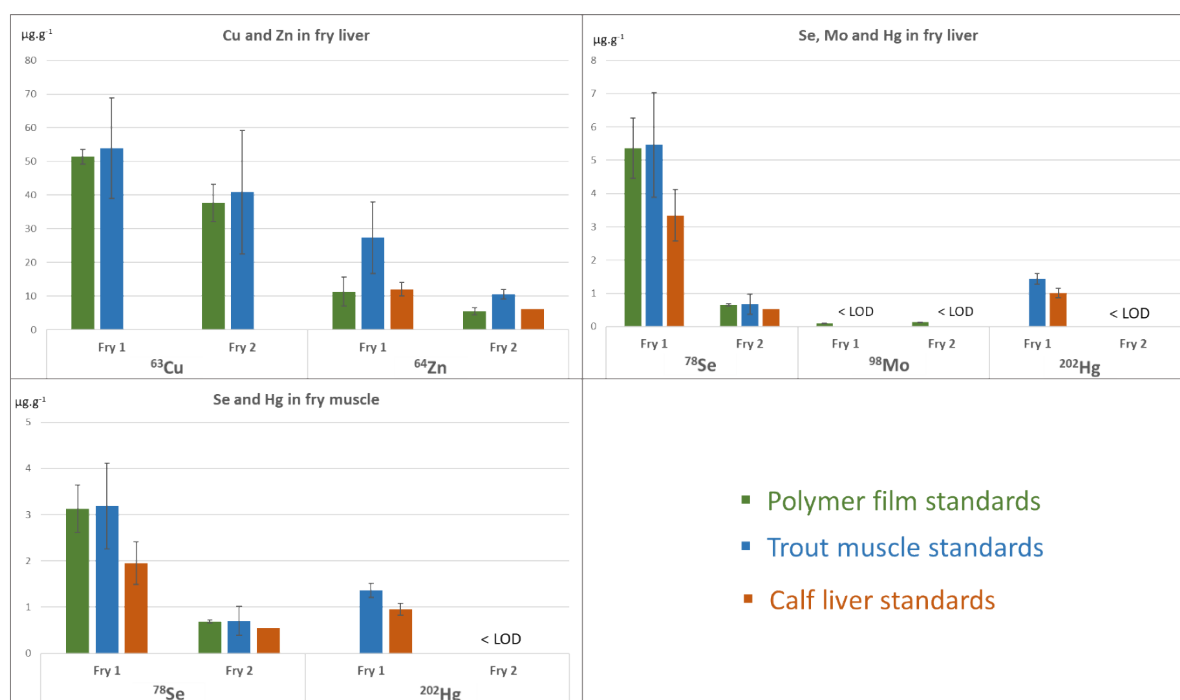


Fig. 6. Concentrations determined for each element by the polymer film method (green), the trout muscle standards (blue) and the calf liver standards (orange) in fry liver (top graphs) and in fry muscle (bottom graph). Mean of concentrations obtained with calibration analysed before and after the sample analysis, and the corresponding SD (only one calibration for the second fry quantification).

Fry liver and muscle signals were more precisely quantified by integrating signals on selected area (**Fig. 6**). In the liver, Cu was 10 $\mu\text{g}\cdot\text{g}^{-1}$ lower for fry 2 compared to fry 1. Similarly, concentrations twice lower were found for fry 2 for Zn. There was not an important difference in Mo concentration between both fry with 0.10 $\mu\text{g}\cdot\text{g}^{-1}$ (fry 1) and 0.14 $\mu\text{g}\cdot\text{g}^{-1}$ (fry 2) determined by the polymer film method (below LOD with MMS). However, as we can clearly see in **Fig. 5**, Se and Hg concentration (5 $\mu\text{g}\cdot\text{g}^{-1}$ and 1.4 $\mu\text{g}\cdot\text{g}^{-1}$ for Se and Hg, respectively) were higher in fry 1 directly supplemented in SeMet and MeHg compared to fry 2 (around 0.7 $\mu\text{g}\cdot\text{g}^{-1}$ for Se and < LOD for Hg). The same difference was visible in the fry muscles, with Se twice more concentrated in fry 1, and Hg present at around 1 $\mu\text{g}\cdot\text{g}^{-1}$. There was less bias between the two concentrations when the quantification is done with the polymer calibration (lower SDs), compared to the MMS for all elements (except for Zn with calf liver standards). For Cu, the mean values were similar between polymer films and trout muscle standards quantification, with only 3% and 6% of difference for fry 1 and the fry 2, respectively. For Se, means values were very similar between polymer films and trout muscle standards (1% difference), whereas the concentration obtained with calf liver standard was lower (25% (fry 1) and 14% (fry 2) difference). For Hg, a difference of 25% was obtained between muscle and liver standards for fry 1 (fry 2 < LOD). For Zn, concentrations determined by polymer films and liver standards were closed, whereas the value obtained with muscle standards was twice higher. For Mo, concentrations determined in the liver with MMS were below

LOD. However, when quantifying the maximum Mo concentrations in the digestive tract with MMS, differences between the three methods were of 21% for fry 1 and 26% for fry 2.

Depending on the element, the polymer films quantification was similar to the trout muscle standards quantification (Cu and Se), to the calf liver standards quantification (Zn) or similar between the three (Mo).

4 Conclusion

Two methodologies (i.e polymer film and matrix-matched standards) were developed for the quantitative imaging of Se, Hg Cu, Zn and Mo in entire rainbow trout fry. Both methodologies offer advantages while some drawbacks can be noticed. First, homogeneous polymer films could be produced on large glass slides (4 cm x 4 cm), substrate needed for entire fry deposit and allowing internal standardization. Except for Hg, the polymer film methodology was validated for all elements using two types of home-made matrix-matched standards (MMS). Hg quantitative imaging required the use of the MMS methodology. For endogenous elements such as Cu and Zn, the nature of the MMS is of paramount importance as it can naturally contain these elements (i.e Cu in liver) or may provoke matrix effects such as for Zn in trout muscle. Due to better trace elements purity and homogeneity of polymer film than MMS, elements LOD range of the polymer film were lower than for MMS (0.06-5 $\mu\text{g.g}^{-1}$ vs 0.3-30 $\mu\text{g.g}^{-1}$). The methodologies allowed for the first time the quantification of Se and Hg in entire fry, which is required analytical tool to determine assimilation of these two elements present in aquafeeds.

5 Acknowledgments

The authors thank the E2S project for the funding of the PhD grant of L. Labeyrie. Aquitaine Region and Feder are acknowledged for funding the laser ablation system through the AQUITRACE project. This project has also received funding from the European Union's Horizon 2020 Research and Innovation Programme under the Marie Skłodowska-Curie Grant Agreement no. 101007962. The authors wish to thank Orffa (Breda, The Netherlands) for the kind supply of selenomethionine.

6 References

- [1] M.P. Rayman, The importance of selenium to human health, *The Lancet*. 356 (2000) 233–241. [https://doi.org/10.1016/S0140-6736\(00\)02490-9](https://doi.org/10.1016/S0140-6736(00)02490-9).
- [2] S. Fontagné-Dicharry, S. Godin, H. Liu, P. Antony Jesu Prabhu, B. Bouyssière, M. Bueno, P. Tacon, F. Médale, S.J. Kaushik, Influence of the forms and levels of dietary selenium on antioxidant status and oxidative stress-related parameters in rainbow trout (*Oncorhynchus mykiss*) fry, *Br J Nutr*. 113 (2015) 1876–1887. <https://doi.org/10.1017/S0007114515001300>.
- [3] P. Wischhusen, C. Arnaudguilhem, M. Bueno, G. Vallverdu, B. Bouyssièrè, M. Briens, P. Antony Jesu Prabhu, P.-A. Geraert, S.J. Kaushik, B. Fauconneau, S. Fontagné-Dicharry, S. Mounicou, Tissue localization of selenium of parental or dietary origin in rainbow trout (*Oncorhynchus mykiss*) fry using LA-ICP MS bioimaging, *Metallomics*. 13 (2021) mfaa008. <https://doi.org/10.1093/mtomcs/mfaa008>.
- [4] N.V.C. Ralston, L.J. Raymond, Dietary selenium's protective effects against methylmercury toxicity, *Toxicology*. 278 (2010) 112–123. <https://doi.org/10.1016/j.tox.2010.06.004>.
- [5] H. Pan, L. Feng, Y. Lu, Y. Han, J. Xiong, H. Li, Calibration strategies for laser ablation ICP-MS in biological studies: A review, *TrAC Trends in Analytical Chemistry*. 156 (2022) 116710. <https://doi.org/10.1016/j.trac.2022.116710>.

- [6] M.A.O. da Silva, M.A.Z. Arruda, Laser ablation (imaging) for mapping and determining Se and S in sunflower leaves, *Metallomics*. 5 (2013) 62–67. <https://doi.org/10.1039/C2MT20154B>.
- [7] D.J. Hare, J. Lear, D. Bishop, A. Beavis, P.A. Doble, Protocol for production of matrix-matched brain tissue standards for imaging by laser ablation-inductively coupled plasma-mass spectrometry, *Anal. Methods*. 5 (2013) 1915. <https://doi.org/10.1039/c3ay26248k>.
- [8] D. Clases, S. Fingerhut, A. Jeibmann, M. Sperling, P. Doble, U. Karst, LA-ICP-MS/MS improves limits of detection in elemental bioimaging of gadolinium deposition originating from MRI contrast agents in skin and brain tissues, *Journal of Trace Elements in Medicine and Biology*. 51 (2019) 212–218. <https://doi.org/10.1016/j.jtemb.2018.10.021>.
- [9] M. Šala, V.S. Šelih, J.T. van Elteren, Gelatin gels as multi-element calibration standards in LA-ICP-MS bioimaging: fabrication of homogeneous standards and microhomogeneity testing, *Analyst*. 142 (2017) 3356–3359. <https://doi.org/10.1039/C7AN01361B>.
- [10] H.-J. Stärk, R. Wennrich, A new approach for calibration of laser ablation inductively coupled plasma mass spectrometry using thin layers of spiked agarose gels as references, *Anal Bioanal Chem*. 399 (2011) 2211–2217. <https://doi.org/10.1007/s00216-010-4413-1>.
- [11] C. Austin, D. Hare, T. Rawling, A.M. McDonagh, P. Doble, Quantification method for elemental bio-imaging by LA-ICP-MS using metal spiked PMMA films, *J. Anal. At. Spectrom*. 25 (2010) 722. <https://doi.org/10.1039/b911316a>.
- [12] C. Arnaudguilhem, M. Larroque, O. Sgarbura, D. Michau, F. Quenet, S. Carrère, B. Bouyssière, S. Mounicou, Toward a comprehensive study for multielemental quantitative LA-ICP MS bioimaging in soft tissues, *Talanta*. 222 (2021) 121537. <https://doi.org/10.1016/j.talanta.2020.121537>.
- [13] M. Bonta, H. Lohninger, M. Marchetti-Deschmann, A. Limbeck, Application of gold thin-films for internal standardization in LA-ICP-MS imaging experiments, (2014) 11.
- [14] C. Austin, F. Fryer, J. Lear, D. Bishop, D. Hare, T. Rawling, L. Kirkup, A. McDonagh, P. Doble, Factors affecting internal standard selection for quantitative elemental bio-imaging of soft tissues by LA-ICP-MS, *J. Anal. At. Spectrom*. 26 (2011) 1494. <https://doi.org/10.1039/c0ja00267d>.
- [15] J.S. Becker, R.C. Dietrich, A. Matusch, D. Pozebon, V.L. Dressler, Quantitative images of metals in plant tissues measured by laser ablation inductively coupled plasma mass spectrometry, (2008) 5.
- [16] D.A. Frick, D. Günther, Fundamental studies on the ablation behaviour of carbon in LA-ICP-MS with respect to the suitability as internal standard, *J. Anal. At. Spectrom*. 27 (2012) 1294. <https://doi.org/10.1039/c2ja30072a>.
- [17] D.J. Bellis, R. Santamaria-Fernandez, Ink jet patterns as model samples for the development of LA-ICP-SFMS methodology for mapping of elemental distribution with reference to biological samples, *J. Anal. At. Spectrom*. 25 (2010) 957. <https://doi.org/10.1039/b926430b>.
- [18] R. González De Vega, M.L. Fernández-Sánchez, J. Pisonero, N. Eiró, F.J. Vizoso, A. Sanz-Medel, Quantitative bioimaging of Ca, Fe, Cu and Zn in breast cancer tissues by LA-ICP-MS, *Journal of Analytical Atomic Spectrometry*. 32 (2017) 671–677. <https://doi.org/10.1039/c6ja00390g>.

- [19] I. Moraleja, M.L. Mena, A. Lázaro, B. Neumann, A. Tejedor, N. Jakubowski, M.M. Gómez-Gómez, D. Esteban-Fernández, An approach for quantification of platinum distribution in tissues by LA-ICP-MS imaging using isotope dilution analysis, *Talanta*. 178 (2018) 166–171. <https://doi.org/10.1016/j.talanta.2017.09.031>.
- [20] N. Grijalba, A. Legrand, V. Holler, C. Bouvier-Capely, A novel calibration strategy based on internal standard–spiked gelatine for quantitative bio-imaging by LA-ICP-MS: application to renal localization and quantification of uranium, *Anal Bioanal Chem*. 412 (2020) 3113–3122. <https://doi.org/10.1007/s00216-020-02561-4>.
- [21] S. Braeuer, T. Van Helden, T. Van Acker, O. Leroux, D. Van Der Straeten, A. Verbeken, J. Borovička, F. Vanhaecke, Quantitative mapping of mercury and selenium in mushroom fruit bodies with laser ablation–inductively coupled plasma-mass spectrometry, *Analytical and Bioanalytical Chemistry*. 414 (2022) 7517–7530. <https://doi.org/10.1007/s00216-022-04240-y>.
- [22] M. Iwase, Y. Tanaka, N. Suzuki, Y. Ogra, Determination of spatial mercury concentration by laser ablation-inductively coupled plasma mass spectrometry, *The Journal of Toxicological Sciences*. 46 (2021) 193–198. <https://doi.org/10.2131/jts.46.193>.
- [23] G. Counotte, M. Holzhauser, S. Carp-van Dijken, J. Muskens, D. Van der Merwe, Levels of trace elements and potential toxic elements in bovine livers: A trend analysis from 2007 to 2018, *PLoS ONE*. 14 (2019) e0214584. <https://doi.org/10.1371/journal.pone.0214584>.
- [24] R.J.A. Goodwin, A. Nilsson, D. Borg, P.R.R. Langridge-Smith, D.J. Harrison, C.L. Mackay, S.L. Iverson, P.E. Andrén, Conductive carbon tape used for support and mounting of both whole animal and fragile heat-treated tissue sections for MALDI MS imaging and quantitation, *Journal of Proteomics*. 75 (2012) 4912–4920. <https://doi.org/10.1016/j.jprot.2012.07.006>.
- [25] I. Blanco-Penedo, J.M. Cruz, M. López-Alonso, M. Miranda, C. Castillo, J. Hernández, J.L. Benedito, Influence of copper status on the accumulation of toxic and essential metals in cattle, *Environment International*. 32 (2006) 901–906. <https://doi.org/10.1016/j.envint.2006.05.012>.
- [26] D.P. Bishop, D. Clases, F. Fryer, E. Williams, S. Wilkins, D.J. Hare, N. Cole, U. Karst, P.A. Doble, Elemental bio-imaging using laser ablation-triple quadrupole-ICP-MS, *J. Anal. At. Spectrom*. 31 (2016) 197–202. <https://doi.org/10.1039/C5JA00293A>.
- [27] D. Pozebon, V.L. Dressler, M.F. Mesko, A. Matusch, J.S. Becker, Bioimaging of metals in thin mouse brain section by laser ablation inductively coupled plasma mass spectrometry: novel online quantification strategy using aqueous standards, *J. Anal. At. Spectrom*. 25 (2010) 1739. <https://doi.org/10.1039/c0ja00055h>.
- [28] K. Billimoria, D.N. Douglas, G. Huelga-Suarez, J.F. Collingwood, H. Goenaga-Infante, Investigating the effect of species-specific calibration on the quantitative imaging of iron at mg kg⁻¹ and selenium at µg kg⁻¹ in tissue using laser ablation with ICP-QQQ-MS, *J. Anal. At. Spectrom*. 36 (2021) 1047–1054. <https://doi.org/10.1039/D1JA00042J>.
- [29] M. Debeljak, J.T. van Elteren, K. Vogel-Mikuš, Development of a 2D laser ablation inductively coupled plasma mass spectrometry mapping procedure for mercury in maize (*Zea mays* L.) root cross-sections, *Analytica Chimica Acta*. 787 (2013) 155–162. <https://doi.org/10.1016/j.aca.2013.05.053>.
- [30] T. Van Helden, S. Braeuer, T. Van Acker, O. Leroux, D. Van Der Straeten, F. Vanhaecke, High-speed mapping of Hg and Se in biological tissue via laser ablation-inductively coupled plasma-

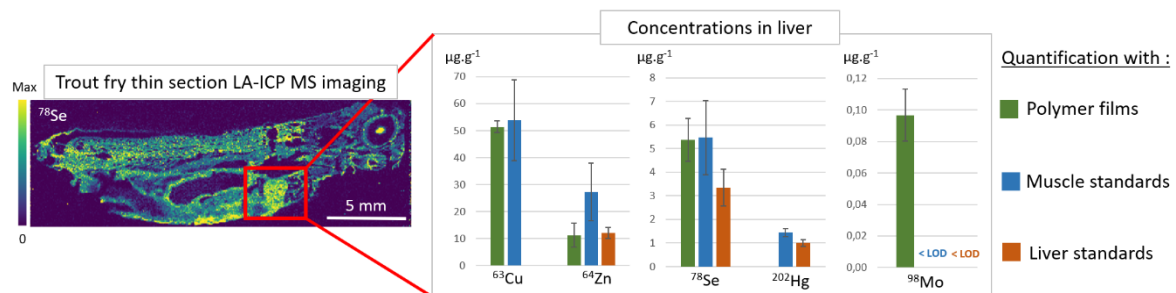
mass spectrometry, *Journal of Analytical Atomic Spectrometry*. 37 (2022) 1455–1461.
<https://doi.org/10.1039/d2ja00131d>.

We confirm that the manuscript has been read and approved by all named authors and that there are no other persons who satisfied the criteria for authorship but are not listed. We further confirm that the order of authors listed in the manuscript has been approved by all of us.

Declaration of interests

The authors declare that they have no known competing financial interests or personal relationships that could have appeared to influence the work reported in this paper.

The authors declare the following financial interests/personal relationships which may be considered as potential competing interests:



Selenium and mercury quantitative imaging in entire rainbow trout fry by LA-ICP MS using polymer films and biological matrices as standards

Laurie Labeyrie¹, Germain Salvato Vallverdu¹, Dominique Michau², Stéphanie Fontagné-Dicharry³, Sandra Mounicou¹

¹Université de Pau et des Pays de l'Adour, E2S UPPA, CNRS, IPREM, Pau, France

²CNRS, Université Bordeaux, ICMCB, UMR 5026, 87 avenue du Dr A. Schweitzer, 33608, Pessac, France

³INRAE, Université de Pau et des Pays de l'Adour, E2S UPPA, NUMEA, 64310 Saint-Pée-sur-Nivelle, France

* Author to whom correspondence should be addressed: sandra.mounicou@univ-pau.fr, IPREM UMR 5254, Technopôle Hélioparc, 2 avenue du Président Angot, 64053 Pau cedex 09, phone: ++33 5 59 40 77 64

Highlights

Development of large size polymer film substrates for quantitative LA-ICP MS imaging

Development of a matrix-matched standards based quantitative LA-ICP MS imaging

Comparison of the methodology's performances and validation

Quantitative LA-ICP MS imaging of Se, Hg, Cu, Zn and Mo in entire trout fry